

CAVITATION UNDER MAGNETIC FIELD: STUDY OF AN OSCILLATING BUBBLE

Y. Bouzehouane, F. Ayela, O. Budenkova

Univ. Grenoble Alpes, CNRS, Grenoble INP, LEGI, 38610 Grenoble, France

This study investigates the influence of a non-uniform static magnetic field on bubble dynamics during cavitation, focusing specifically on bubble oscillation. Using a numerical simulation approach, we applied a magnetic field to a low pressure bubble inside a large volume of fluid to follow oscillation of the bubble’s radius neglecting liquid–gas mass exchange. Our simulations showed impacts of the magnetic field on the bubble dynamics slightly affecting the minimum bubble radius and implosion dynamics. This modification might be related to the shock wave modification.

Introduction.

Cavitation involves the formation and growth of vapor pockets. This phenomenon arises due to phase changes in the liquid, triggered by a drop in pressure below the fluid’s vaporization point. When the low-pressure condition is relieved, the vapor pocket is fractured into multiple bubbles, then the bubbles collapse, i.e. shrink to an extremely small size, but they can rebound, i.e. expand again. Thus, the disappearance of a bubble is preceded by its oscillation between implosion (extremal shrinking) and expansion. The implosion results in a significant increase in temperature and pressure of the internal gas, along with an increase of velocity of the bubble’s surface. The high velocity of the bubble’s surface generates shock waves, whose interaction with the surrounding materials causes erosion of the latter. Additionally, the increase in pressure and temperature can ionise the gas, i.e. form plasma and produce hydroxyl radicals [1, 2]. The ionization of the gas inside the bubble results in luminescence, therefore, luminescence can be used to detect the bubble’s implosion. The light emitted from the bubble provides a means to obtain information about the bubble around its minimum radius. In single-bubble sonoluminescence experiments with water, Young *et al.* [3] observed that applying a strong magnetic field (between 1 and 10 T) shifted the acoustic pressure range, within which the bubble implodes with luminescence toward higher values. They hypothesized that the magnetic field generates non-uniform forces along the bubble interface, thereby perturbing successive rebounds and breaking the symmetry, which in turn may affect the maximum temperature and pressure reached.

Most studies on the application of magnetic fields to two-phase flows, particularly cavitation, have focused on electrically conductive fluids, where inductive effects presumably play a significant role in the observed phenomena [4, 5]. However, for paramagnetic and diamagnetic non-conducting fluids, effects of a non-uniform magnetic field \mathbf{B} due to a volume force known as the Kelvin force given by Eq. (1) can be expected:

$$\mathbf{f}_{\text{vol mag}} = \frac{\chi}{2\mu_0} \nabla (\mathbf{B}^2). \quad (1)$$

Here, χ is the magnetic susceptibility of the medium [6]. The effect of the Kelvin force is analogous to that of the hydrostatic pressure variation and may induce convective flow in media with the spatially varying χ . The deformation of the interface between two

phases [7] or the magnetophoretic separation in particle-laden flows [8] are examples of the effect of the Kelvin force.

One can find only a few studies regarding the effect of the magnetic field on the cavitating flow of paramagnetic fluids. The study by Shalobasov and Shal'nev [9] demonstrated that applying a magnetic field transverse to the flow direction in a cavitating water around a cylinder resulted in an increase in both the mass loss due to erosion and the affected surface area. They attributed these effects to the interaction between the magnetic field and an ionic layer at the bubbles' interface. Later, Shal'nev *et al.* [10] observed an increase in spark-generated bubble growth rates in the presence of a magnetic field, resulting in bubbles with a larger maximum radius, but the implosion phase was not addressed. Hammitt [11] has shown that erosion could increase or decrease depending on the magnetic field's direction and the specifics of the experimental system. Then, Kamiyama *et al.* [12] noted that a 0.6 T magnetic field in acoustic cavitation caused damage over a larger area, though it was less severe. Yet, nor the direction of the magnetic field neither its gradient were specified. Recently, in the field of biology, Yang *et al.* [13] explored the relationship between acoustic cavitation and blood-brain barrier opening (BBBO). This technique uses cavitation to open the brain barrier near its surface by focusing acoustic waves. Preliminary studies showed a reduction in cavitation level under a 9.4 T magnetic field compared to conditions without the field, which was corroborated by further studies with magnetic fields intensity of 1.5 T, 3 T, and 4.7 T [14].

In the present work, we study numerically whether a magnetic field affects bubble implosion or rebound, focusing only on bubble dynamics and excluding chemical effects and possible interactions of the magnetic field with ionized gas.

1. Description of a two-dimensional numerical model.

The feasibility of modelling of bubble implosion using Volume-of-Fluid (VOF) implementation in ANSYS Fluent was demonstrated elsewhere [15] provided a very fine mesh is used to avoid numerical artefacts, and the computation domain is large enough to avoid the effect of boundaries. Following the aforementioned approach, a two-dimensional axially symmetric domain with a circular external boundary is considered, the size of the domain is taken 100 times larger than the initial maximum size of the bubble which is equal to $1 \cdot 10^{-4}$ m, the centre of the bubble coincides with the geometrical centre of the domain, and the strategy with a block-structured mesh is adopted for the mesh construction (Fig. 1). A constant pressure of 1 atm equal to the initial pressure in the liquid is imposed at the boundary of the computation domain that allows the liquid to freely leave and enter the domain. The region, where the variation of the magnetic field is considered in the calculations is bounded by the two red dotted lines shown in Fig. 1, outside that region the magnetic field is assumed to be constant. It is supposed that the magnetic field is generated by a magnet at the left of the figure. One may consider the left red line be corresponding to the surface of a magnet that generates the magnetic field $B_{an}(x, y)$ decreasing along the symmetry axis of the domain that is presented with an analytical function. The components of the volume force given by Eq. (1) are introduced into the corresponding momentum equations given below via User Defined Functions. It should be noted that the magnetic susceptibility of fluids are supposed to be linearly dependent on the fluid density $\chi = \chi_0 \rho / \rho_0$, with $\chi_0 = -9.035 \cdot 10^{-6}$ [16] being the base value for water and $\rho_0 = 998.8 \text{ kg/m}^3$. This approximation is a way of accounting for the decrease in the number of atoms in a given volume and, therefore, the decrease in the number of electrons reacting with the magnetic field.

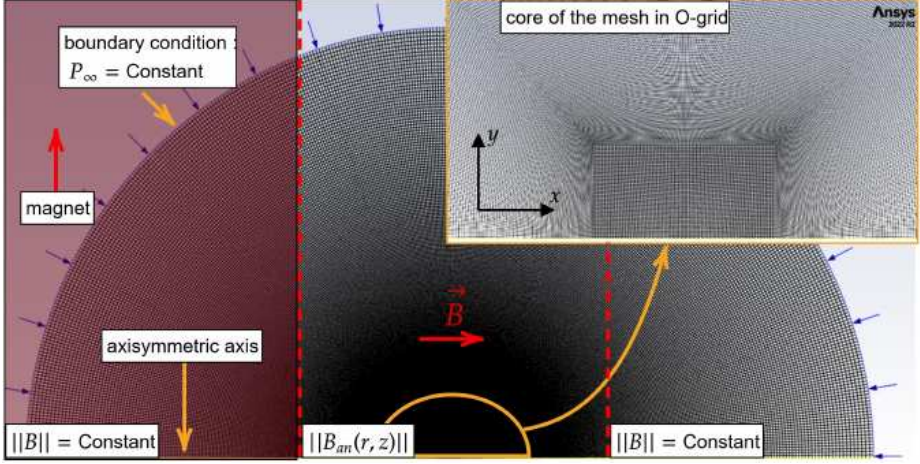


Fig. 1. Illustration of the mesh and indication of boundary conditions.

In the model, both fluids are assumed to be viscous and compressible with a polytropic equation of state for the gas and the following compressible liquid state equation for the liquid $(\rho_1/\rho_{l,0})^n = K_0 + n(p - p_0)/K_0$, with p being the pressure, ρ_1 the density of the liquid phase, $K_0 = 2.1 \cdot 10^9$, $\rho_{l,0} = 998.2 \text{ kg/m}^3$, $n = 7.12$ and $p_0 = 1 \text{ atm}$.

Further, with the VOF approach, for all fluids in the system a single set of momentum and energy equations is used (as presented below), while the presence of a phase i in each calculation cell is defined with use of a volume fraction α_i . The properties in hydrodynamic and energy equations are calculated using linear mixture laws as described elsewhere [17]. The continuity equation with \mathbf{u} for the velocity is

$$\partial_t \rho + \nabla(\rho \mathbf{u}) = 0.$$

The momentum equation is

$$\partial_t(\rho \mathbf{u}) + \nabla(\rho \mathbf{u} \otimes \mathbf{u}) = -\nabla P + \nabla \cdot \tau + \mathbf{f}_{\text{vol mag}},$$

with P standing for the pressure, and the stress τ is defined as

$$\tau = \mu[\nabla \mathbf{u} + (\nabla \mathbf{u})^T] - 2/3\mu(\nabla \cdot \mathbf{u})\mathbb{I}.$$

The volume fraction is calculated using the following equation for the secondary phase which is represented in the model by gas, with the fraction α_g and a partial velocity \mathbf{u}_g :

$$\partial_t(\alpha_g \rho_g) + \nabla(\alpha_g \rho_g \mathbf{u}_g) = 0.$$

The energy E is calculated using the following equation, where k represents the thermal conductivity:

$$\partial_t E + \nabla \left(\rho \mathbf{u} \left(E + \frac{p}{\rho} \right) \right) = \nabla(k \nabla T).$$

2. Results.

The VOF-based numerical model for the bubble implosion was verified by comparing with the Keller–Miksis model presented in the next section. A spherically-symmetric geometry does not allow the introduction of a non-uniform magnetic field which would

correspond to a real physical situation, yet the Keller–Miksis model serves for the verification of a numerical case implemented in ANSYS Fluent using the VOF approach. Then the VOF model was used to study the effect of the magnetic field introduced in the problem.

2.1. Comparison with a Keller–Miksis problem. We have modelled a spherical bubble oscillation using the Keller–Miksis framework [18, 19], which describes a bubble in a viscous liquid collapsing or expanding due to the pressure difference inside and outside the bubble, ΔP . The liquid follows the fluid-gas interface, where the surface tension is taken into account, but the phase transformation is not considered, and both phases are assumed to be homogeneous. The model neglects the appearance of shock waves, the heat exchange between the two phases and neglects the density of the gas relative to that of the liquid. With the outlined assumptions, the variation of the bubble radius R over time is described by Eqs. (2)–(3) derived from the mass and momentum conservation equation for the radial component of the velocity. Eq. (4) is the state equation for the gas.

$$\left(1 - \frac{\dot{R}}{c}\right) R\ddot{R} + \frac{3}{2}\dot{R}^2 \left(1 - \frac{\dot{R}}{3c}\right) = \left(1 + \frac{\dot{R}}{c}\right) \frac{1}{\rho_l} (P_{\text{int}}(R) - P_\infty) + \frac{R}{c\rho_l} \dot{P}_{\text{int}}, \quad (2)$$

$$P_{\text{int}}(R) = P_{\text{bubble}}(R) - \frac{2\sigma}{R} - 4\mu_l \frac{\dot{R}}{R}, \quad (3)$$

$$P_{\text{bubble}} = P_0 (R_0/R)^{3\gamma}. \quad (4)$$

Here, the first and second time derivatives \dot{R} , \ddot{R} correspond to the velocity and acceleration of the bubble surface motion, ρ_l , μ_l , c are, respectively, the liquid density, dynamic viscosity and the speed of sound in the liquid, P_{int} is the pressure at the interface of the bubble, P_{bubble} is the pressure inside the bubble, and σ is the surface tension.

For the comparison, the following parameters were used: $p_{g0} = 6900$ Pa is the initial pressure inside the bubble, $R_0 = 10^{-4}$ m is the initial radius of the bubble, $p_{\text{bound}} = 1$ atm is the pressure at the domain’s boundary, with the gas properties in the simulation being set to those of the air. The gas properties were chosen to match those of the air to satisfy the condition $\rho_g \ll \rho_l$, where ρ_g is the gas density. The bubble radius in time obtained from the solution of Eqs. (2)–(4) performed using a Matlab code is shown in Fig. 2 (black line).

A similar problem was solved with ANSYS Fluent with the time step adjusted to have a Courant number equal to 0.05. The momentum, density and energy equation were resolved with second-order schemes and the convergence criteria for continuity, energy, volume fraction of fluid, the X and Y velocity is such that the relative normalised error is below 10^{-3} , 10^{-6} , 10^{-4} , 10^{-4} and 10^{-4} , respectively. To extract the radius of a bubble from the distribution of the volume fraction obtained with the VOF-based model, we considered a set of points, whose liquid fraction satisfies the inequality $0.4 < \alpha_1 < 0.6$. Then the error between these points and the circle equation was minimized, allowing determining the coordinates of the bubble center and the bubble radius. If the bubble is deformed, the method gives an equivalent bubble radius, whose variation is shown in Fig. 2 (brown line).

The difference in the bubble radius after rebound between the two models can be attributed to the fact that in the VOF model the assumption of uniform gas temperature is ignored, and the temperature distribution in the bubble is calculated. According to

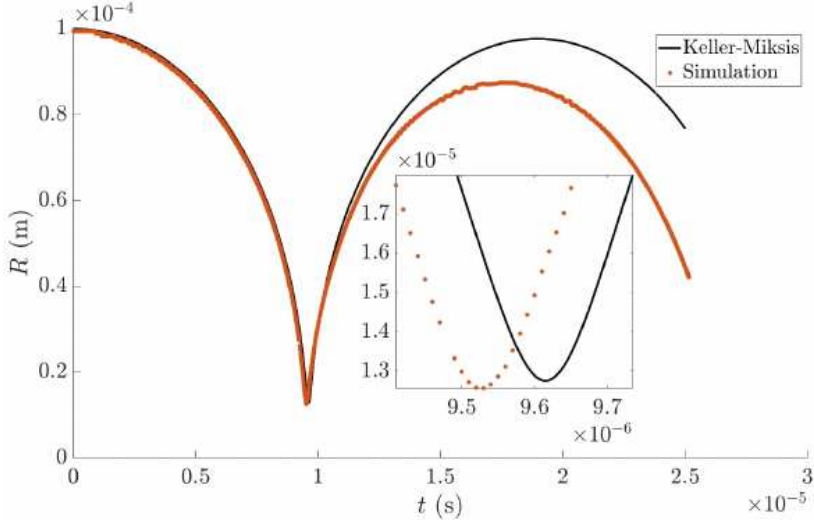


Fig. 2. The bubble radius over time calculated for the Keller–Miksis model with Eqs. (2)–(4) and with the ANSYS Fluent VOF model with the air properties for the gas inside the bubble.

the discussion in [20], the presence of a thermal layer between the two phases appears to radically alter the bubble’s energy dissipation, making the rebound weaker and shorter. Overall, a very good agreement was observed until the bubble implosion (maximum shrinking). The minimum value of the radius which is $\sim 1.25 \cdot 10^{-5}$ m in the ANSYS Fluent model and $\sim 1.28 \cdot 10^{-5}$ m in the solution for the Keller–Miksis equations has a relatively small relative difference of 2.3%. The observed discrepancy can be assigned to the absence of shock wave effects in the Keller–Miksis model and to the heat exchange between the bubble and the liquid taken into account in the VOF model, but not in the Keller–Miksis model. Nevertheless, the results obtained with the VOF-based model have appeared physically plausible and describe rather well the bubble implosion. It is also noted that the time associated with the minimum radius of the bubble exhibits a small variation between the two simulations.

2.2. Magnetic field effect on bubble implosion.

The simulation was performed with the adopted VOF-based model using the following parameters: $p_{g0} = 6900$, $R_0 = 10^{-4}$ m, $p_{\text{bound}} = 1$ atm, with the gas properties set to those of water vapor. Three cases were considered: without a magnetic field, a magnetic field $|B| = 4$ T with the gradient $\nabla(|B|) = 1000$ T/m and a magnetic field of $|B| = 8$ T with the corresponding gradient $\nabla(|B|) = 2000$ T/m. Fig. 3 shows the variation of the bubble radius over time for different magnetic field intensities. Only the most intense magnetic field used in the simulation has provided visible effects on the bubble dynamics.

These effects that appear with a slight delay of the bubble implosion and a higher value of the minimum radius of the bubble seem minor. However, the maximum deviation between the simulations with and without the magnetic field equivalent to 8 T is $\Delta R/R_0 = 7\%$ and the decelerated dynamics result in a temporal shift of 3%. The temporal shift is becoming increasingly significant during the cycle of growth and the second collapse of the bubble, especially after $t = 2.5 \cdot 10^{-5}$ s the gap is clearly visible. The effect of the magnetic field on the eventual bubble deformation can be estimated by the Bond

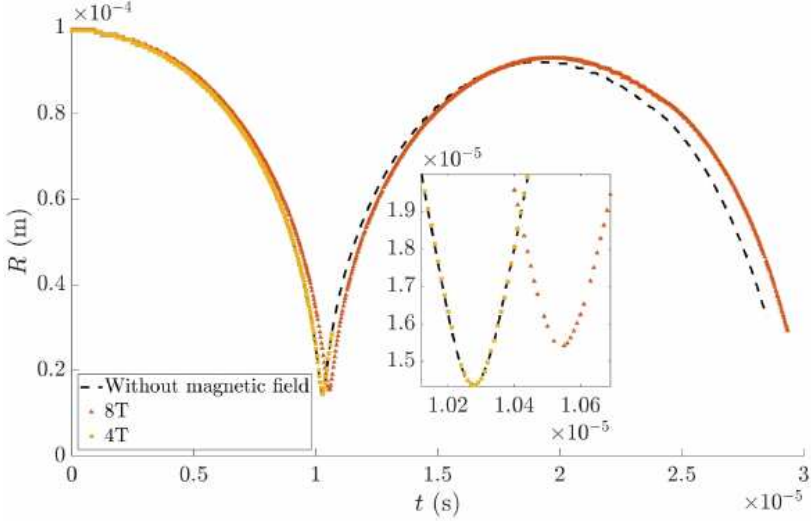


Fig. 3. Radius as the function of time for the simulation without a magnetic field and with a magnetic field equivalent to $B = 4$ T and $B = 8$ T with $R_0 = 10^{-4}$ m and water vapor properties for the gas inside the simulation.

number [21]:

$$Bo_{\text{mag}} = \frac{\chi R_0 \mathbf{B}_{\text{eq}}^2}{2\mu_0\sigma},$$

that, for the initial value of the bubble radius and the maximum intensity of the magnetic field gives $Bo_{\text{mag}} \sim 0.3$. This means that the magnetic pressure on the bubble is low compared with the surface tension, and, if an effect exist, it can be small and that is actually confirmed by the numerical modeling.

As it was mentioned above, during the implosion, the rapid movement of the bubble surface initiates pressure waves and shock waves that propagate through the fluid and reflect off the bubble interface. The Mach number $Ma = |\mathbf{u}_{\text{max}}|/c$, with c standing for the local speed of sound, determines whether the shock wave can appear in the problem, that is expected if $Ma > 0.7$. In the problem, the maximum speed of the bubble surface just before or after the implosion, $t = 6.23 \cdot 10^{-6}$ s and $t = 8.87 \cdot 10^{-6}$ s, is 60 m/s that gives Ma up to 0.77, if c is taken for the gas-liquid mixture under 1 bar [22]. These shock waves and pressure waves travel radially outward, gradually attenuating as they move away from the bubble, as presented in Fig. 4 with the contour of the density gradient $\nabla\rho$ near the bubble. This figure highlights the effect of the magnetic field on the pressure variation which is initiated by the waves propagating throughout the domain during the bubble's oscillations. A minor effect of the magnetic field is observed when comparing Figs. 4 (b) and (e), but a significant change in patterns is noticeable between (c) and (f).

Thorough examination of the bubble's interface defined by the water vapor fraction $0.4 < \alpha_{\text{vapor}} < 0.6$ has revealed a weak deformation of the bubble because of the imposed magnetic field that causes the shock waves generated at the interface to overlap in the certain regions as they no longer retain spherical symmetry. This alteration in the shock wave patterns appears to reduce the compression of the bubble at its minim radius compared to cases, where only the magnetic field pressure effect is considered.

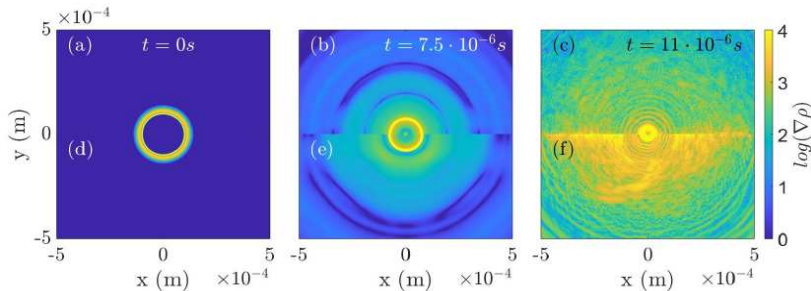


Fig. 4. Logarithm of the density gradient in the near-bubble domain for three different times. (a), (b) and (c) for the contour without a magnetic field, and (d), (e) and (f) for a magnetic field equivalent to 8 T.

3. Discussion.

Only minor effects of the magnetic field on the dynamics of the imploding bubble was found. The results obtained in the current work cannot be immediately applied to the single-bubble luminescence experiments mentioned in the Introduction, as additional phenomena should be taken into account. However, the work should be considered as a preliminary stage for further, more complex modeling. This stage allowed us to understand the constraints of the model which may entail discrepancies between numerical results and experimental observations. Among these constraints, the most important probably is the fact that the plasma formation is not considered, therefore, the direct effect of the magnetic field on the electrical charges is not taken into account. It should be also noted that another effect of the magnetic field which modifies the pressure on the bubble in the presence of the magnetic field is considered in the work of Yasui [23]. This pressure modification is derived from the energy conservation equation and is related to the work which the magnetic field performs by constantly orienting the polar molecules along the magnetic lines against their disorientation due to thermal vibration. The estimations performed in [23] provides a significantly stronger effect of the magnetic pressure than the one obtained in the current work with Eq. (1) and accepted values for the magnetic permeability. However, this estimation is determined by the value of a coefficient related to the probability of molecular disorientation, which is not known. In fact, this coefficient was estimated from the single cavitating bubble experiment. Moreover, the cited work has not considered other phenomena related to cavitation, that are the dissipation of energy due to viscosity of the fluid and the appearance of the shock waves.

Conclusions.

It should be emphasised that a careful consideration must be given to discretization schemes and time-step selection to avoid errors due to insufficient convergence in numerical modeling. The computational mesh should be as structured as possible, adapting to different spatial scales according to the bubble’s evolution stage. This adaptive approach is essential for achieving optimal resolution, from the initial bubble size to the bubble’s implosion. Implementing an “O-grid” structure enhances this resolution capability and helps avoiding the artificial deformation of the liquid–gas interface as it passes through different meshes.

Introducing a magnetic field into a cavitation model reveals alterations in bubble dynamics, particularly concerning the bubble implosion and shock wave behavior. Our findings emphasize the influence of magnetic fields on the increase of the minimum bubble radius and a delay of implosion. These effects can be attributed to the interactions

between the magnetic field and the shock wave. While our simulations yield physically plausible results, some discrepancies between numerical simulations and experimental observations are expected due to inherent model simplifications. The present study highlights the impact of magnetic fields on cavitation dynamics, laying the ground for further research and experimental validation. Advanced numerical techniques and structured meshing are essential for achieving reliable simulation outcomes, and ongoing refinement of the models will improve our understanding of the cavitation phenomena under the influence of magnetic fields. Future research should consider incorporating polarized layer effects and plasma dynamics into numerical simulations of cavitation under magnetic fields, as these phenomena are particularly sensitive to magnetic influence.

Acknowledgments.

The authors wish to acknowledge the funding support of “Carnot Energies du Future” and of the Grenoble Alpes University via the programme “IRGA”.

References

- [1] R. PFLIEGER, H.P. BRAU AND S.I. NIKITENKO. Sonoluminescence from $\text{OH}(C^2\Sigma^+)$ and $\text{OH}(A^2\Sigma^+)$ radicals in water: Evidence for plasma formation during multibubble cavitation. *Chemistry – A European Journal*, vol. 16 (2010), pp. 11801–11803.
- [2] K. PENG, S. SHOUCENG, Y. ZHANG, Q. HE, Q. WANG. Penetration of hydroxyl radicals in the aqueous phase surrounding a cavitation bubble. *Ultrasonics Sonochemistry*, vol. 91 (2022), p. 106235.
- [3] J.B. YOUNG, T. SCHMIEDEL, AND KANG WOOWON. Sonoluminescence in high magnetic fields. *Phys. Rev. Lett.*, vol. 77 (1996), pp. 4816–4819.
- [4] R.G. PEREL'MAN AND E.V. GOVORSKII. Effect of a constant magnetic field on cavitation erosion in an electrically conducting liquid. *Soviet Physics Doklady*, vol. 16 (1971), p. 164.
- [5] S. KAMIYAMA AND T. YAMASAKI. Cavitation in a flow of mercury in a transverse magnetic field. *Magnetohydrodynamics*, vol. 10 (1974), no. 3, pp. 277–280.
- [6] T.A. BUTCHER AND J.M.D. COEY. Magnetic forces in paramagnetic fluids. *Journal of Physics: Condensed Matter*, vol. 35 (2022), p. 53002.
- [7] S. UENO AND M. IWASAKA. Properties of diamagnetic fluid in high gradient magnetic fields. *Journal of Applied Physics*, vol. 75 (1994), pp. 7177–7179.
- [8] F. SHIRI, H. FENG AND B.K. GALE. Chapter 14: Passive and active microfluidic separation methods. In: *Particle Separation Techniques*, (2022), pp. 449–484.
- [9] I.A. SHALOBASOV AND K.K. SHAL'NEV. Effect of an external magnetic field on cavitation and erosion damage. *Heat Transfer-Sov. Res.*, vol. 3 (1971), p. 032110.
- [10] K.K. SHAL'NEV, I.A. SHALOBASOV, S.P. KOZYREV AND E.V. KHALDEEV. Cavitation bubble in magnetic field. In: *Proc. the 5th Conference on Fluid Machinery*, vol. 2 (1975), pp. 1021–1028.

- [11] F.G. HAMMITT, E. YILMAZ, O. AHMED, N.R. BHATT AND J. MIKIELEWICZ. Effects of magnetic and electric fields upon cavitation in conducting and non-conducting liquids. In: *Proc. 1975 ASME Polyphase Flow Forum*, 1974, p. 22643.
- [12] S. KAMIYAMA, K. KOIKE AND H. KAWAGUCHI. Effects of a magnetic field on cavitation damage: Experiments in tap water. *Bulletin of JSME*, vol. 25 (1982), pp. 1690–1695.
- [13] Y. YANG, C. PACIA, D. YE, Y. YUE, C. CHIEN AND H. CHEN. Static magnetic fields dampen focused ultrasound-induced cavitation and blood-brain barrier opening outcome. *The Journal of the Acoustical Society of America*, vol. 150 (2021), pp. A29–A30.
- [14] Y. YANG, C. PACIA, D. YE, Y. YUE, C. CHIEN AND H. CHEN. Static magnetic fields dampen focused ultrasound-mediated blood-brain barrier opening. *Radiology*, vol. 300 (2021), pp. 681–689.
- [15] P. KOUKOUVINIS, M. GAVAISES, O. SUPPONEN AND M. FARHAT. Numerical simulation of a collapsing bubble subject to gravity. *Physics of Fluids*, vol. 28 (2016), p. 032110.
- [16] G.P. ARRIGHINI, M. MAESTRO AND R. MOCCIA. Magnetic properties of polyatomic molecules. I. Magnetic susceptibility of H_2O , NH_3 , CH_4 , H_2O_2 . *The Journal of Chemical Physics*, vol. 49 (1968), pp. 882–889.
- [17] Y.R. SIVATHANU AND G.M. FAETH. Generalized state relationships for scalar properties in nonpremixed hydrocarbon/air flames. *Combustion and Flame*, vol. 82 (1990), pp. 211–230.
- [18] J.B. KELLER AND I.I. KOLODNER. Damping of underwater explosion bubble oscillations. *Journal of Applied Physics*, vol. 27 (1956), pp. 1152–1161.
- [19] J.B. KELLER AND M. MIKSIS. Bubble oscillations of large amplitude. *The Journal of the Acoustical Society of America*, vol. 68 (1980), pp. 628–633.
- [20] X. ZHONG, J. ESHRAGHI, P. VLACHOS, S. DABIRI AND A.M. ARDEKANI. A model for a laser-induced cavitation bubble. *International Journal of Multiphase Flows*, vol. 132 (2020), p. 103433.
- [21] Y. LI, X. D. NIU, A. KHAN, D.C. LI AND H. YAMAGUCHI. A numerical investigation of dynamics of bubbly flow in a ferrofluid by a self-correcting procedure-based lattice Boltzmann flux solver. *Physics of Fluids*, vol. 31 (2019), p. 082107.
- [22] S.W. KIEFFER. Sound speed in liquid-gas mixtures: Water-air and water-steam. *Journal of Geophysical Research*, vol. 82 (1977) pp. 2895–2904.
- [23] K. YASUI. Effect of a magnetic field on sonoluminescence. *Phys. Rev. E*, vol. 60 (1999), pp.1759–1761.

Received 11.12.2024